Journal of Coordination Chemistry

ISSN: (Print) (Online) Journal homepage: https://www.tandfonline.com/loi/gcoo20

Microwave-assisted synthesis and DNA-binding studies of half-sandwich ruthenium(II) arene complexes containing phenanthroimidazole-triarylamine hybrids

Ramakrishnan Abhijna Krishna, Ramachandran Dheepika, Mathiyan Muralisankar & Samuthira Nagarajan

To cite this article: Ramakrishnan Abhijna Krishna, Ramachandran Dheepika, Mathiyan Muralisankar & Samuthira Nagarajan (2021) Microwave-assisted synthesis and DNA-binding studies of half-sandwich ruthenium(II) arene complexes containing phenanthroimidazole-triarylamine hybrids, Journal of Coordination Chemistry, 74:4-6, 838-849, DOI: 10.1080/00958972.2021.1885650

To link to this article: https://doi.org/10.1080/00958972.2021.1885650

JOURNAL OF COORDINATION CHEMISTRY
2021, VOL. 74, NOS. 4–6, 838–849
https://doi.org/10.1080/00958972.2021.1885650

Taylor & Francis
Taylor & Francis Group

Microwave-assisted synthesis and DNA-binding studies of half-sandwich ruthenium(II) arene complexes containing phenanthroimidazole-triarylamine hybrids

Ramakrishnan Abhijna Krishna, Ramachandran Dheepika, Mathiyan Muralisankar and Samuthira Nagarajan

Department of Chemistry, Central University of Tamil Nadu, Thiruvarur, India

ABSTRACT

A new series of half-sandwich Ru(II)-arene complexes with phenanthroimidazole-triarylamine hybrid ligands were synthesized and scrutinized for DNA binding studies. The metal complexes were prepared via microwave-assisted synthesis with high yield and purity. The interaction of Ru(II)-arene complex with calf thymus DNA was studied by spectrophotometric methods. All six complexes exhibited significant interaction with CT-DNA. Methoxyphenyl-substituted metal complex showed the highest binding efficiency with a binding constant (K_b) of 5.053×10^4 M^{-1} due to its electron-rich nature. The methoxyphenyl group remarkably enhanced the interaction through stabilization of π-orbital of the metal complex which resulted in the efficient coupling. Phenyl- and thiophene-substituted ligands also showed good binding constants of 4.908×10^4 M^{-1} and 4.509×10^4 M^{-1}, respectively. The absorption and ethidium bromide displacement studies declare that both the intercalation and groove binding is anticipated by these complexes. These Ru(II) complexes with phenanthroimidazole-triarylamine hybrid ligands can be realized as efficient DNA binding agents.

ARTICLE HISTORY
Received 2 August 2020
Accepted 2 January 2021

KEYWORDS
Ruthenium(II) arene; phenanthroimidazole; triarylamine; DNA-binding

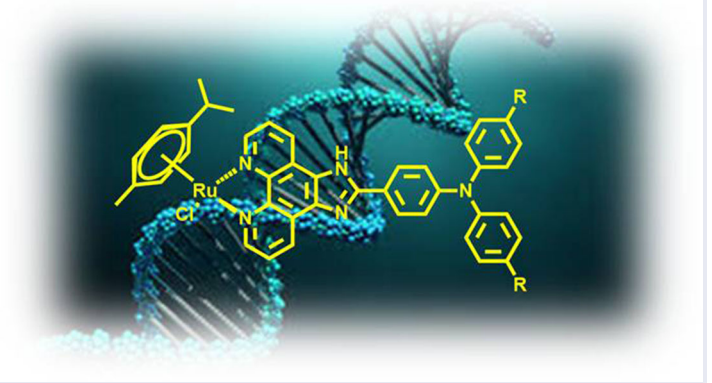

CONTACT Samuthira Nagarajan snagarajan@cutn.ac.in Department of Chemistry, Central University of Tamil Nadu, Thiruvarur, 610005, India

Supplemental data for this article is available online at https://doi.org/10.1080/00958972.2021.1885650.

1. Introduction

Revolution in cancer therapy was heralded by the discovery of cisplatin in 1965 [1, 2]. Cytotoxicity induced by platinum drugs is due to the cross-linking of DNA and thereby inhibiting the replication and protein synthesis. However, severe side-effects like neurotoxicity, renal toxicity, myelo suppression, ototoxicity, hair loss, and poor solubility of the drug in the liquid medium have restricted the applications [3–5]. As an alternative, owing to the excellent physicochemical properties, ruthenium complexes are now receiving attention as potent anticancer agents [6]. Two of the complexes such as sodium salt of indazolium [*trans*-[tetrachloridobis(1H-indazole)ruthenate(III)] (KP1339) and imidazolium [*trans*-tetrachlorido(dimethylsulfoxide)(1H-imidazole)ruthenate(III)] (NAMI-A) have successfully reached the stage of human trials [7]. Ru(II)-*p*-cymene-PTA complex is also progressing towards the clinical trials [8]. These complexes are beneficial over platinum complexes as they possess similar binding nature as iron and antimetastatic as well [9]. Also, ruthenium complexes have become a promising class of metallodrugs because of their excellent DNA-binding properties and their good interaction with the blood proteins. The solubility of complexes with blood proteins provides an easier path for transportation and protects the complexes against premature elimination or degradation [10]. Besides, modification of Ru complexes with different ligand systems gives the effective change in treating a diverse type of tumor. Hence, global research is focusing on different applications of ruthenium complexes with various biologically significant ligands [11].

In the background of developing good DNA-binding agents containing Ru, the 'piano-stool' skeleton of half-sandwich Ru(II)-arene complexes offer many possibilities to modify the structural characteristics and biological action of the complexes, which leads to possible antiproliferative activity towards tumor cells [12, 13]. Additionally, the piano-stool confirmation of Ru(II) arene complexes allows it to show a variety of catalytic applications like closing olefin metathesis [14], C(sp^2)-H activation of substituted pyridines [15], oxidation of alcohols [16], and asymmetric catalysis for Diels–Alder reactions [17]. Dyson and Aird *et al.* developed half-sandwich ruthenium complexes having similar ligand exchange properties as that of platinum (II) anticancer drugs [18, 19]. According to them, the biological activities of complexes are decided by the nature of chelating arene ligands. Gianferrara *et al.* [20] classified metal anticancer compounds based on their mode of action and categorized them into groups of functional compounds. The activity of complexes depended on the type of metal center, its electronic configuration, oxidation state, and its hard-soft nature. Isostructural piano-stool complexes with different metal ions have been studied for their biological activity [21, 22]. The Ru(II) compound (RM175) and its osmium(II) analog (AFAP51) displayed significant variations *in vitro* and *in vivo* anticancer activities. Casini and co-workers demonstrated that Rh(III) and Ir(III) complexes are inactive towards anticancer activity by comparing the CpRh(III) and CpIr(III) derivatives and osmium complexes of RAPTA-C to the NAMI-A Ru(III) complex [23]. The enhanced stability of half-sandwich Ru(II) complexes with heterocycles due to hydrogen bonding plays an important role in the anticancer mechanism [24]. In the absence of stable hydrogen bond interactions, dissociation of

the ligand occurs in the solution, confirmed by NMR spectroscopic studies. Hydrogen-bonding based structure-activity relationship has modified the drug action mechanism at the cellular and molecular levels [25, 26].

The present work came from our continuous interests in studying the chemotherapeutic activity of half sandwiched ruthenium(II) complexes. 1,10-Phenanthroline (phen) is a typical chelating bidentate ligand that shows novel properties by coordinating to different transition metals [27–29]. It is a heteroaromatic system having beautifully placed nitrogen atoms acting cooperatively, with remarkable characters such as rigidity, planarity, hydrophobicity, and electron deficiency [30, 31]. Triarylamine (TAA) derivatives exhibit various pharmacological activities. Organometallic half-sandwich Ir(III) complexes containing TAA substituted bipyridyl ligands were able to oxidize NADH to NAD^+ efficiently and they showed good binding property to DNA and bovine serum albumin [32]. They hold an exceptional mode of interaction with DNA and are exclusively bound to quadruplex DNA [33, 34]. Imidazole is important in the field of medicinal chemistry as it is a constituent in biologically important molecules like histidine, histamine, biotin, alkaloids, nucleic acids, *etc.* and has shown anticancer activity [35, 36].

In this investigation, we have designed and synthesized six new half-sandwich ruthenium(II) arene complexes containing phen-TAA hybrids. The metal complexes were synthesized by focused microwave-assisted reaction with high purity and yield. Interaction modes of the complexes with DNA have been investigated by UV-Vis absorption and emission spectroscopic techniques. The binding and cleavage properties of phen-metal complexes were modulated by functionalization of the phen unit. The introduction of electron-rich substituents on the TAA side influences the rate of interaction with CT-DNA.

2. Experimental

2.1. Materials and methods

All reagents and solvents were purchased from commercial sources and used as received without purification. $[RuCl_2(\eta^6\text{-}p\text{-cymene})]_2$ was synthesized as per the literature method [37]. Phen-TAA hybrids were newly synthesized in our research laboratory [38]. ^1H and ^{13}C NMR spectra were collected on a Bruker 400 MHz spectrometer in $CDCl_3$. Mass spectral analysis was performed on a Thermo Scientific Exactive Plus UHPLC MS spectrometer. FT-IR spectra were recorded on a Perkin Elmer spectrometer. UV-Vis spectra were acquired on a Jasco spectrophotometer. Emission spectra were obtained from the Perkin Elmer spectrophotometer. Thermogravimetric analyses were done on a Perkin Elmer thermogravimetric analyzer with a ramp rate of 10 °C per minute from 30 to 800 °C under an N_2 atmosphere.

2.2. Synthesis of metal complexes

$[Ru(\eta^6\text{-}p\text{-cymene})Cl_2]_2$ was prepared by dissolving 0.5 g of ruthenium(III) chloride in 25 mL of ethanol and sonicated for 15 min in a round bottom flask. α-Pellandrene (4 mL) was added to the reaction mixture, stirred to get a clear solution, and consequently refluxed for four hours. The obtained clear red solution was kept in the deep

freezer for 2 days. The obtained reddish-brown crystals were washed with methanol and dried in vacuum to get a 76% yield of $[Ru(\eta^6\text{-}p\text{-cymene})Cl_2]_2$.

TAA aldehydes were initially synthesized as per the procedure reported [39]. The phen-TAA hybrid ligands were prepared by heating a mixture of 1,10-phenanthroline-5,6-dione (5 mmol), ammonium acetate (100 mmol), corresponding TAA aldehydes (6 mmol), and glacial acetic acid (4 mL) at 100 °C in 250 watt for about 20 min in a CEM microwave synthesizer. The reaction mixture was poured into ice to get a yellow precipitate and was collected by filtration using Whatman 40 filter paper. The precipitate was washed with ammonia solution to neutralize and consequently, washed with hot water. The precipitate was dried to get yellow solid in 98% yield.

$[(C_6H_6)RuCl_2]_2$ (0.1 mmol) and phen-TAA ligands (0.2 mmol) in 12 mL of dichloromethane were allowed to react in a CEM microwave synthesizer for 30 min (pre-stirring: 2 min., temperature: 60 °C, power: 250 watt, pressure: 275 PSI). The addition of hexane to the reaction mixture gave an orange-yellow solid. The solid was collected by filtration, washed with hexane several times, and air-dried to get 91% of the product.

$[(\eta^6\text{-}p\text{-}cym)Ru^{II}(1)(Cl)]Cl$, 7: Yield: 95%. ESI-MS Calcd for $C_{41}H_{35}Cl_2N_5Ru$ $[M\text{-}Cl]^+$, 734.162; found, 734.144. ^{1}H NMR (400 MHz, $CDCl_3$) δ (ppm): 13.731 (s, 1H), 13.1539 (d, J = 5.6 Hz, 1H), 12.192 (d, J = 5.6, 1H), 11.985 (d, J = 12.4 Hz, 1H), 11.868 (s, 1H), 11.267 (t, J = 6.8 Hz, 3H), 11.0875 (m, 6H), 10.1265 (d, J = 5.2 Hz, 1H), 9.345 (d, J = 5.6 Hz, 1H), 6.500 (s, 6H), 6.214 (s, 3H), 5.180 (s, 3H), 5.790 (d, J = 5.6 Hz, 6H), 3.930 (s, 1H). ^{13}C NMR (100 MHz, $CDCl_3$) δ (ppm): 145.81, 128.41, 126.87, 124.23, 122.84, 120.73, 102.99, 83.05, 38.79, 32.89, 29.55, 20.79, 17.93.

$[(\eta^6\text{-}p\text{-}cym)Ru^{II}(2)(Cl)]Cl$, 8: Yield: 90%. ESI-MS Calcd for $C_{55}H_{47}Cl_2N_5O_2Ru$ $[M\text{–}Cl]^+$, 946.246; found, 946.242. ^{1}H NMR (400 MHz, $CDCl_3$) δ (ppm): 14.78 (s, 1H), 9.505 (s, 2H), 8.958 (s, 2H), 8.376 (s, 3H), 7.798 (s, 1H), 7.695 (s, 1H), 7.492 (s, 1H), 7.216 (s, J = 6.8 Hz, 4H), 6.952 (d, J = 7.6 Hz, 4H), 5.902 (m, 3H), 2.616 (s, 1H), 2.229 (s, 4H), 1.862 (s, 6H), 1.256 (s, 3H), 0.932 (s, 6H).^{13}C NMR (100 MHz, $CDCl_3$) δ (ppm): 158.95, 149.40, 145.54, 143.40, 136.18, 136.21, 133.21, 128.61, 128.02, 127.61, 126.01, 125.51, 125.41, 122.19, 114.19, 113.20, 86.47, 86.97, 83.97, 55.34, 31.07, 30.90, 29.69, 22.05, 18.83.

$[(\eta^6\text{-}p\text{-}cym)Ru^{II}(3)(Cl)]Cl$, 9: Yield: 92%. ESI-MS Calcd for $C_{49}H_{39}Cl_2N_5S_2Ru$ $[M\text{-}Cl]^+$, 898.137; found, 898.135. ^{1}H NMR (400 MHz, $CDCl_3$) δ (ppm): 15.026 (s, 1H), 10.169 (s, 1H), 9.501 (d, J = 19.6 Hz, 2H), 9.108 (s, 1H), 8.476 (s, 2H), 7.868 (s, 1H), 7.744 (s, 1H), 7.511 (d, J = 7.6 Hz, 4H), 7.386 (m, 6H), 7.11 (d, J = 6.8 Hz, 3H), 5.909 (m, 2H), 2.935 (m, 1H), 2.636 (s, 1H), 2.227 (s, 2H), 1.725 (s, 2H), 1.256 (s, 3H), 0.954 (s, 6H). ^{13}C NMR (100 MHz, $CDCl_3$) δ (ppm): 145.96, 141.77, 131.30, 128.71, 127.50, 126.22, 125.41, 122.56, 119.66, 86.45, 84.24, 9931.17, 29.97, 21.97, 18.84.

$[(\eta^6\text{-}p\text{-}cym)Ru^{II}(4)(Cl)]Cl$, 10: Yield: 91%. ESI-MS Calcd for $C_{53}H_{43}Cl_2N_5Ru$ $[M\text{–}Cl]^+$, 886.225; found, 886.232. ^{1}H NMR (400 MHz, $CDCl_3$) δ (ppm): 14.921 (s, 1H), 10.099 (s, 1H), 9.563 (d, J = 10 Hz, 3H), 9.081 (s, 1H), 8.482 (s, 1H), 7.854 (s, 1H), 7.737 (s, 1H), 7.581 (d, J = 6.8 Hz, 3H), 7.520 (d, J = 7.2 Hz, 3H), 7.421 (t, J = 6.4 Hz, 3H), 7.335 (m, 2H), 7.227 (d, J = 6.4 Hz), 5.919 (m, 4H), 2.612 (s, 1H), 2.194 (s, 2H), 1.928 (s, 3H), 1.257 (s, 3H), 0.921 (s, 6H). ^{13}C NMR (100 MHz, $CDCl_3$) δ (ppm): 145.96, 141.77, 131.30, 127.50, 126.22, 25.41, 122.56, 119.66, 86.45, 84.24, 31.17, 29.70, 21.97, 18.87.

$[(\eta^6\text{-}p\text{-}cym)Ru^{II}(5)(Cl)]Cl$, 11: Yield: 89%. ESI-MS Calcd for $C_{41}H_{33}Cl_2I_2N_5Ru$ $[M\text{-}Cl]^+$, 985.955; found, 985.982. ^{1}H NMR (400 MHz, $CDCl_3$) δ (ppm): 15.097 (s, 1H), 10.222 (s,

1H), 9.561 (s, 1H), 9.483 (s, 1H), 9.174 (s, 1H), 8.513 (s, 1H), 7.910 (s, 1H), 7.780 (s, 1H), 7.564 (d, J = 6.8 Hz, 4H), 7.138 (d, *J* = 6.8 Hz, 1H), 6.881 (d, *J* = 7.2 Hz, 2H), 5.913 (m, 3H), 2.675 (s, 1H), 2.246 (s, 2H), 1.675 (s, 6H), 1.255 (s, 3H), 0.982 (s, 3H). ^{13}C NMR (100 MHz, $CDCl_3$) δ (ppm): 148.38, 146.55, 143.75, 138.63, 128.90, 126.74, 123.28, 86.97, 31.16, 29.70, 22.19, 22.03.

[(η^6-*p*-cym)Ru^{II}(6)(Cl)]Cl, 12: Yield: 92%. ESI-MS Calcd for $C_{65}H_{59}Cl_2N_5Ru$ $[M\text{-}Cl]^+$, 1046.350; found, 1046.356. ^{1}H NMR (400 MHz, $CDCl_3$) δ (ppm): 15.052 (s, 1H), 10.197 (s, 1H), 9.613 (s, 1H), 9.131 (s, 1H), 8.573 (s, 1H), 8.506 (s, 1H), 7.903 (m, 3H), 7.456 (t, *J* = 6.8 Hz, 5H), 7.456 (t, J = 6.8 Hz, 5H), 7.366 (d, J = 5.6 Hz, 4H), 7.222 (d, J = 7.2 Hz, 2H), 7.099 (d, J = 9.2 Hz, 3H), 5.904 (m, 3H), 4.199 (s, 1H), 2.658 (s, 1H), 2.236 (s, 3H), 1.803 (s, 3H), 1.324 (s, 18H), 0.960 (s, 6H). ^{13}C NMR (100 MHz, $CDCl_3$) δ (ppm): 151.42, 132.84, 131.32, 129.12, 125.64, 124.39, 120.35, 34.80, 34.44, 31.37, 31.20, 29.70, 22.17, 22.04, 18.95.

2.3. DNA interaction studies

UV-Vis Absorption and fluorescence studies: The interaction mode of complexes with CT-DNA was explored by UV-vis absorption and fluorescence emission studies. The experiments were performed in 50 mMNaCl/5 mM trisHCl (pH 7.2) solution at room temperature. The calf-thymus DNA (CT-DNA) was prepared by sonicating it in tris-HCl/NaCl buffer for three days at 4 °C and stored at 4 °C. The DNA was free of proteins as indicated by the absorption ratio 1.9 of the stock solution of CT-DNA at λ_{max} 260 and 280 nm. Ten-fold dilution of the bulk DNA solution was done to show maximum absorbance at 260 nm with the absorption coefficient value of 6600 $M^{-1}cm^{-1}$ per nucleotide. The titration experiments were made by keeping the complex concentration constant (5 μM) and varying the CT-DNA concentration (20–50 μM). Samples were equilibrated before recording each spectrum [40, 41] and a significant absorbance change was noticed. The intrinsic binding constant (K_b) of the complexes with CT-DNA was quantitatively calculated from the following equation to compare the effect of different substitutions [41]:

$$\frac{[DNA]}{(\varepsilon_a - \varepsilon_f)} = [DNA]/(\varepsilon_b - \varepsilon_f) + 1/K_b(\varepsilon_b - \varepsilon_f)$$

where [DNA] = concentration of DNA in base pairs, ε_a (apparent extinction coefficient) = observed absorbance/[complex] and ε_f (extinction coefficient for free complex) = absorbance for blank solution/[complex]. K_b was calculated from the plot of $[DNA]/(\varepsilon_a - \varepsilon_f)$ *versus* [DNA] by taking the ratio of the slop and the intercept. The competitive binding study of the metal complexes with a known intercalator, ethidium bromide (EB), was conducted to further understand the binding mode of complexes with CT-DNA. EB solution was prepared in Tris-HCl/NaCl buffer. The change in fluorescence emission intensity at 599 nm was recorded.

3. Results and discussion

The metal complexes were designed with the three coordination sites of ruthenium in $[(\eta^6\text{-arene})Ru^{II}(X)(Y)(Z)]^+$ is occupied by the arene moiety and the other ligands occupy

the rest three coordination sites which resemble the piano stool. The arene group provides a hydrophobic nature to the complex that helps it to enter the cells by stabilizing +2 oxidation state of the ruthenium. The phen unit of the ligand is highly capable of making chelation with the metal ions. TAA substitution together with the formation of imidazole moiety in the phen unit enhances the DNA binding activity of the metal complex.

The phen-TAA hybrids (**1–6**) were newly synthesized (Scheme 1) and systematically characterized. The complexes [(η^6-*p*-cymene)Ru(η^2-*N*,*N*-L)Cl]Cl (L = **1–6**) were synthesized from phen-TAA hybrids (**1–6**) and [$RuCl_2(\eta^6$-*p*-cymene)]$_2$ precursors in 2:1 molar ratio in DCM at 60 °C in a CEM microwave synthesizer. All the complexes are orange-yellow solids, air-stable, non-hygroscopic, and highly soluble in chloroform, dichloromethane, dimethylformamide, dimethylsulphoxide, methanol, and acetonitrile.

3.1. FT-IR and NMR characterization

IR absorption observed in the range 1583–1617 cm^{-1} and 1456–1569 cm^{-1} corresponds to the groups ν(C=N) and ν(C=C), respectively. A negative shift of ~60 cm^{-1} in ν(C=N) in comparison to the ligand is suggestive of coordination of ruthenium ion is through the nitrogen atoms. The broad band observed in the range 3013–3066 cm^{-1} corresponds to N-H stretching frequency of the ligand. The ^{1}H NMR spectra of complexes were recorded in $CDCl_3$. The aliphatic protons of *p*-cymene moiety were shielded and gave sharp singlets in the range of 0.925–0.985 ppm. Another set of singlets around 1.256–1.800 ppm correspond to the 3H of the *p*-cymene. The N-H signal was observed in the highly deshielded region of 10–15 ppm as compared to that of the ligand N-H protons also supports the coordination of the ligands to metal. In the ^{13}C NMR spectra of the complexes, the signals that appeared around 18–29 ppm and 84–86 ppm were assigned to the aliphatic and aromatic carbon atoms in the *p*-cymene group, respectively. Peaks in the range of 145–158 ppm and 132–149 ppm correspond to the -C = N and -C-N; these peaks appeared to be slightly deshielded from the ligand peaks [11, 38]. The signals for all other protons and carbons were located in the appropriate regions. TGA was done at the ramp rate of 10 °C in the temperature range of 25 to 800 °C. The compounds show a single step of decomposition in the range of 330 to 370 °C and the order of thermal stability was observed to be **9** > **12** > **10** > **8** > **11** > **7**. The high decomposition temperature of

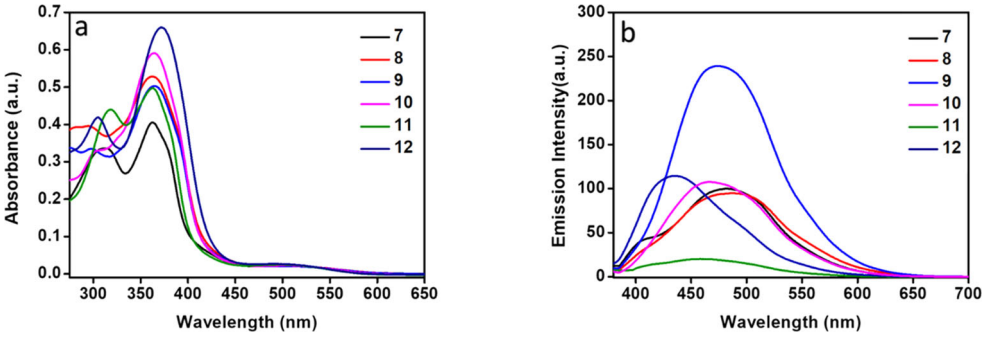

Figure 1. (a) Absorption and (b) emission spectra of **7–12**.

Table 1. Photophysical properties and binding constant values of 7–12.

Complex	λ_{abs} (nm)	λ_{em} (nm)	Stokes' shift (cm^{-1})	Absorption coefficient ε (10^4 M^{-1} cm^{-1})	Binding constant K_b (1×10^4 M^{-1})
7	310, 362	480	6790	4.063	3.487
8	298, 363	487	7014	5.317	5.053
9	298, 364	474	6375	5.022	4.509
10	304, 364	466	6013	5.923	4.908
11	317, 362	463	6026	4.970	4.103
12	304, 371	434	3912	6.603	4.252

thiophene and tert-butylphenylacetylene substituted metal complexes **9** and **12** is due to extended molecular architecture. Metal complexes without substitution **7** and with iodine substitution have the lowest decomposition temperature (thermograms are given in Figure S25).

3.2. Photophysical studies

UV-vis absorption and emission studies were carried out to understand the photophysical behavior of metal complexes. Absorption behavior was investigated in DMF (10^{-5} M) (Figure 1(a)) and data are represented in Table 1. Complexes **7–12** exhibited intraligand π-π^* transition bands around 306–317 nm with a bathochromic shift of 35–18 nm. The absorption band around 364–370 nm corresponds to n-π^* transition and shows a hypsochromic shift of 2–8 nm as compared to the free ligand. This difference occurs because, during complex formation, the orbitals of the nitrogen atom in the formation of molecular bonding levels have variation in energy for π-π^* and n-π^* transitions [42]. A new absorption band around 515–518 nm corresponds to d-d transition of the metal ion electrons. Complex **12** exhibited the highest absorption coefficient (6.603×10^{-4} M^{-1} cm^{-1}) due to the efficient electron delocalization of tert-butylphenyl substituent. Besides, the acetylene group improved electronic distribution. Complexes **8**, **9** and **10** also exhibited good absorbance due to the presence of methoxyphenyl, thiophene, and phenyl groups, respectively, as the substituents capable of enhancing conjugation. Complexes **7** and **11** having **–H** and **–I**, respectively, exhibited poor absorbance due to the lower conjugation and absence of efficient auxochromic groups. All the complexes exhibited a greater absorption coefficient than that of the ligand, due to spin and Laporte allowed ligand to metal charge transition. This explains the change of the transitions towards higher wavelengths [38]. Emission spectra were recorded in DMF (10^{-7} M) and the spectra are presented in Figure 1(b). All the complexes exhibited significant Stokes shifts, as shown in Table 1. The shape of emission spectra is not mirrored images of the absorption spectra, indicating the geometrical changes of the molecule in the excited state [43].

3.3. DNA-binding studies

3.3.1. Electronic absorption studies

UV spectra of the complexes in the presence and absence of CT-DNA are shown in Figure 2. With increase in the concentration of CT-DNA, absorption bands exhibited hypochromism along with a hypsochromic shift of 1–8 nm, suggesting an intimate

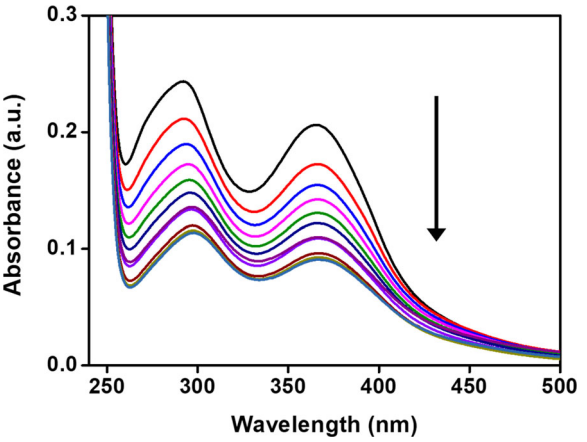

Figure 2. Representative absorption spectra of complexes with CT-DNA in Tris-HCl buffer.

association *via* intercalation [44]. During this process, the π^* orbital of the metal complex will couple with the π orbitals of the base pairs, thereby decreasing the energy of π-π^* transition. Therefore, these interactions resulted in hypochromism [45]. The magnitude of hypsochromic shift and hypochromism indicates the binding strength of complexes [46].

Intrinsic binding constant values are calculated by putting each set of data into the equation $[DNA]/(\varepsilon_a-\varepsilon_f) = [DNA]/(\varepsilon_b-\varepsilon_f) + 1/[K_b(\varepsilon_b-\varepsilon_f)]$. It gave a straight line with a slope of $1/(\varepsilon_b-\varepsilon_f)$ and y-intercept of $1/[K_b(\varepsilon_b-\varepsilon_f)]$ (Table 1, Figure S32). The calculated values of binding constants were in a similar range of other reported complexes [46]. The binding affinity of complexes is the order of **8** > **10** > **9** > **12** > **11** > **7**. The higher binding affinity of methoxyphenyl-substituted TAA-phen complex is due to the tendency to donate electrons to the π^* orbital [44]. This will also stabilize the π^* orbital and reduces the energy gap between the π orbital of DNA and π^* orbital of the metal complex, resulting in efficient coupling [45]. Complex **10** with phenyl substitution has a higher binding constant than thiophene-substituted **9** due to effective delocalization. The unsubstituted metal complex **7** has the lowest binding constant because of the absence of any activating groups. The presence of azole moiety in the ligand can favor the interaction through π–π interaction and H-bonding and thus responsible for the good binding constant values. The higher affinity of imidazole moiety in DNA binding and its anticancer activity has been reported [47].

3.3.2. Fluorescence spectroscopic studies

The studies were carried out in Tris-HCl/NaCl buffer (pH 7.3). The titrations were done by keeping the complex concentration fixed (5 μM) and varying the concentration of CT-DNA (5–45 μM). Since all the complexes were fluorescent in solution, EB was not used for the binding studies [48]. A gradual increase in the emission intensity was observed on the incremental addition of DNA to the complex solution. The enhancement of fluorescence is due to the penetration of the complex into the hydrophobic environment of the DNA, thereby avoiding the quenching effect of solvent water

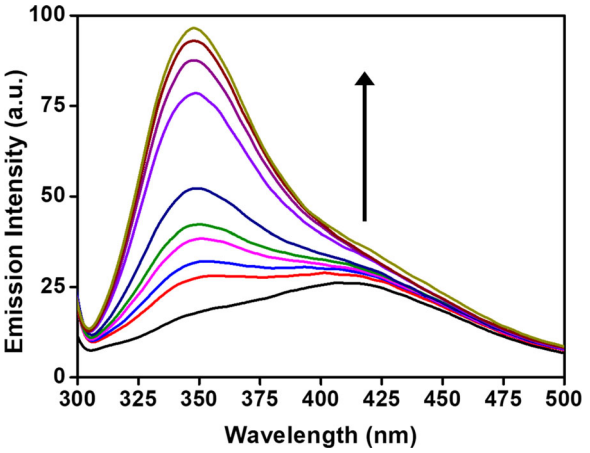

Figure 3. Representative emission spectra of complexes with varying addition of CT-DNA in Tris-HCl buffer.

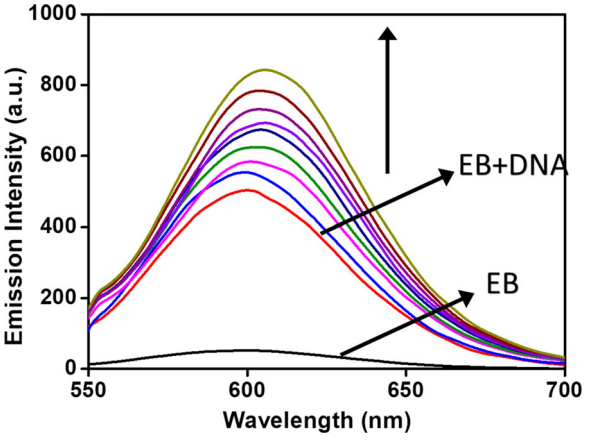

Figure 4. Representative emission spectra of EB bound CT-DNA with the addition of varying concentrations of a metal complex solution.

molecules [49]. This will allow greater electrostatic interaction between the metal complex and DNA in a more rigid and hydrophobic environment with less access to solvent molecules. The marked increase in the emission intensity by the binding of the complex to the CT-DNA agrees with those observed for other intercalators [48]. The hypsochromic shift of 60–67 nm observed for **7–10** may be due to the difference in the mode of interaction of these complexes compared to **11** and **12**. These results show that the complex bound more strongly to the CT-DNA. The emission spectra of complexes with CT-DNA in Tris-HCl buffer is shown in Figure 3.

3.3.3. Comparative binding study with EB

The comparative binding of the metal complex with CT-DNA was performed to understand the binding mode through intercalation or groove binding in nature. The titration was performed by taking a 1:1 ratio of CT-DNA (2.5 μM) and EB (2.5 μM) solution

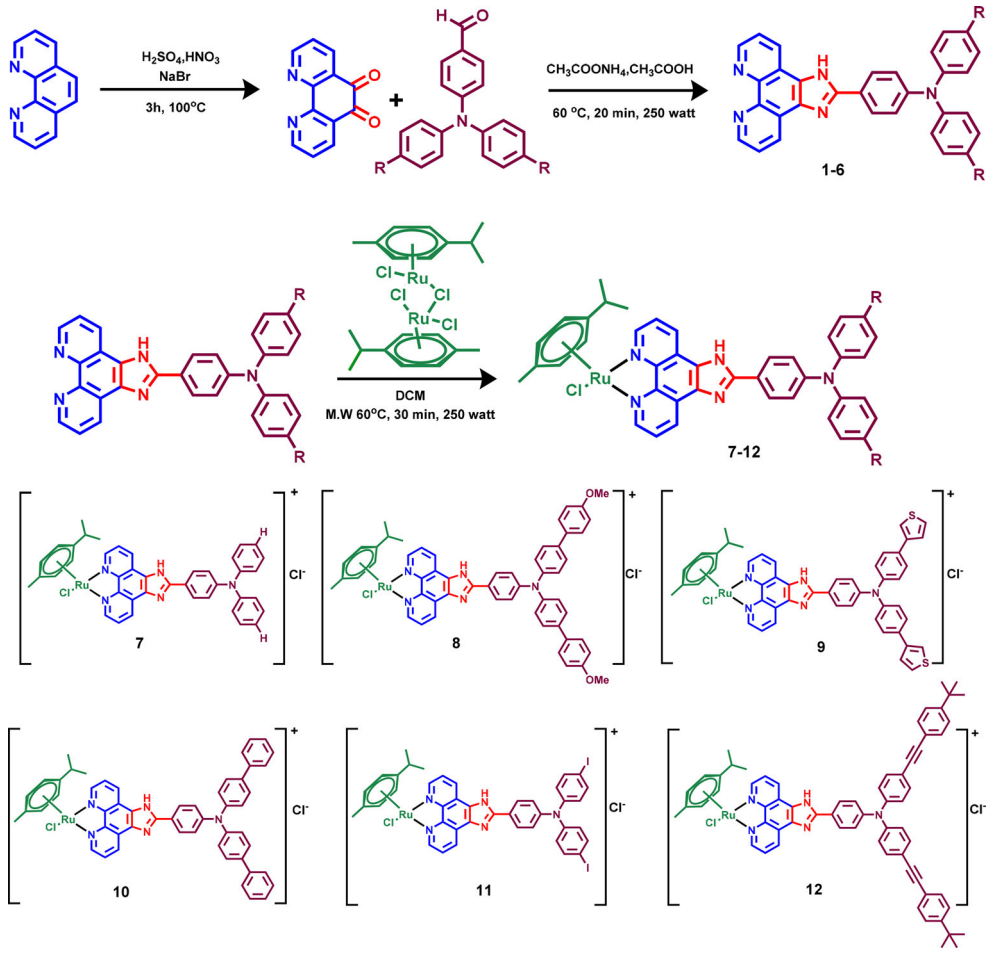

Scheme 1. Synthetic route to phen-TAA hybrid ligands (**1–6**), half-sandwiched Ru(II) arene complexes (**7–12**) and their molecular structure.

and varying concentrations of metal complex solution (2.5–20 μM). The emission intensity was observed to increase gradually on the incremental addition of the metal complex [50]. Thus the experiment shows that the addition of metal complex to the solution does not affect the emission intensity of the EB. This observation confirms that the two probes (EB and CT-DNA) bound independently and do not depend on the other [50]. Thus it reveals that the metal complex also binds through groove-binding to CT-DNA since EB is a known intercalator [51, 52]. The emission spectra of the comparative binding study of EB bound DNA with the metal complex is shown in Figure 4.

4. Conclusion

Six new ruthenium(II) arene complexes containing phenanthroimidazole-TAA hybrid ligands were synthesized using a microwave synthesizer in good yield with high

purity. All the complexes were characterized by analytical and spectral techniques. The metal complex substituted with thiophene is found to be the most thermally stable as observed from TGA studies. Interaction of the complexes with CT-DNA was investigated using UV-vis absorption and fluorescence spectroscopic techniques. UV-Vis absorption studies give information about the intercalative binding of complexes. The binding ability of the complexes was calculated and the methoxyphenyl-substituted was possessing good binding efficiency with a K_b value of 5.053×10^4 M^{-1}. The efficient intercalative binding ability of this complex may be due to its good electron-donating substituent. Emission spectra give information regarding the groove binding nature of complexes. Thus, since our metal complex of interest has several functional centers, it is found to interact with CT-DNA through intercalation as well as groove binding.

Acknowledgement

The authors thank the Central University of Tamil Nadu, Thiruvarur, India for the research facilities.

References

[1] B. Rosenberg, L. Vancamp, T. Krigas. *Nature*, 205, 698 (1965).
[2] B. Rosenberg, L. Vancamp, J.E. Trosko, V.H. Mansour. *Nature*, 222, 385 (1969).
[3] E. Wong, C.M. Giandomenico. *Chem. Rev.*, 99, 2451 (1999).
[4] Z.H. Siddik. *Oncogene*, 22, 7265 (2003).
[5] T. Lazarevic, A. Rilak, Z.D. Bugarcic. *Eur. J. Med. Chem.*, 142, 8 (2017).
[6] L. Zeng, P. Gupta, Y. Chen, E. Wang, L. Ji, H. Chao, Z.S. Chen. *Chem. Soc. Rev.*, 46, 5771 (2017).
[7] E. Alessio, L. Messori. *Molecules*, 24, 1995 (2019).
[8] F. Scalambra, P. Lorenzo-Luis, I. de los Ríos, A. Romerosa. *Eur. J. Inorg. Chem.*, 2019, 1529 (2019).
[9] C.S. Allardyce, P.J. Dyson. *Platinum Met. Rev.*, 45, 62 (2001).
[10] J. Honorato, L.C. Vegas, R.S. Correa, A.P.M. Guedes, M. Miyata, F.R. Pavan, J. Ellena, A.A. Batista. *Inorg. Chem. Front.*, 6, 376 (2019).
[11] J. Palmucci, F. Marchetti, R. Pettinari, C. Pettinari, R. Scopelliti, T. Riedel, B. Therrien, A. Galindo, P.J. Dyson. *Inorg. Chem.*, 55, 11770 (2016).
[12] G. Jaouen, N. Metzler-Nolte (Eds.). *Medicinal Organometallic Chemistry*, Vol. 32, p.21, Springer Verlag, Berlin, Heidelberg (2010).
[13] F. Wang, A. Habtemariam, E.P.L.V. Geer, R. Fernandez, M. Melchart, R.J. Deeth, R. Aird, S. Guichard, F.P.A. Fabbiani, P. Lozano Casal, I.D.H. Oswald, D.I. Jodrell, S. Parson, P.J. Sadler. *Proc. Natl. Acad. Sci. U.S.A.*, 102, 18269 (2005); G. Gasser, I. Ott, N. Metzler-Nolte. *J. Med. Chem.*, 54, 3 (2011).
[14] D. Carmona, M.P. Lamata, F. Viguri, R. Rodríguez, F.J. Lahoz, I.T. Dobrinovitch, L.A. Oro. *Dalton Trans.*, 25, 3328 (2008).
[15] A. Fürstner, A. Fürstner, M. Picquet, C. Bruneau, P.H. Dixneuf. *Chem. Commun.*, 12, 1315 (1998).
[16] K. Singh, J. Singh, H. Singh. *Organometallics*, 27, 4187 (2010).
[17] Y. Boutadla, O. Al-Duaij, D.L. Davies, G.A. Griffith, K. Singh. *Organometallics*, 28, 433 (2009).
[18] P.J. Dyson. *Chimia*, 61, 698 (2007).

[19] R.E. Aird, J. Cummings, A.A. Ritchie, M. Muir, R.E. Morris, H. Chen, P.J. Sadler, D.I. Jodrell. *Br. J. Cancer.*, 86, 1652 (2002).
[20] T. Gianferrara, I. Bratsos, E. Alessio. *Dalton Trans.*, 37, 7588 (2009).
[21] A. Bergamo, A. Masi, A.F. Peacock, A. Habtemariam, P.J. Sadler, G. Sava. *J. Inorg. Biochem.*, 104, 79 (2010).
[22] S.M. Guichard, R. Else, E. Reid, B. Zeitlin, R. Aird, M. Muir, M. Dodds, H. Fiebig, P.J. Sadler, D.I. Jodrell. *Biochem. Pharmacol.*, 71, 408 (2006).
[23] A. Casini, F. Edafe, M. Erlandsson, L. Gonsalvi, A. Ciancetta, N. Re, A. Ienco, L. Messori, M. Peruzzini, P.J. Dyson. *Dalton Trans.*, 39, 5556 (2010).
[24] R. Mitra, S. Das, S.V. Shinde, S. Sinha, K. Somasundaram, A.G. Samuelson. *Chemistry*, 18, 12278 (2012).
[25] S. Das, S. Sinha, R. Britto, K. Somasundaram, A.G. Samuelson. *J. Inorg. Biochem.*, 104, 93 (2010).
[26] L.A. Summers. *Adv. Heterocycl. Chem.*, 1, 22 (1978).
[27] P.G. Sammes, G. Yahioglu. *Chem. Soc. Rev.*, 23, 327 (1994).
[28] C.R. Luman, F.N. Castellano, J.A. McCleverty, T.J. Meyer, A.B.P. Lever. (Eds.), *Compr. Inorg. Chem. II*, 1, 25. 2004
[29] Y. Ooyama, S. Nagano, K. Yoshida. *Tetrahedron*, 65, 1467 (2009); M.S. Tsai, Y.C. Hsu, J.T. Lin, H.C. Chen, C.P. Hsu. *J. Phys. Chem. C*, 111, 18785 (2007).
[30] W.Y. Lin, L.L. Long, L. Yuan, Z.M. Cao, B.B. Chen, W. Tan. *Org. Lett.*, 10, 5577 (2008).
[31] N. Selvakumaran, L. Sandhiya, N.S.P. Bhuvanesh, K. Senthilkumar, R. Karvembu. *New J. Chem.*, 40, 5401 (2016).
[32] X. He, M. Tian, X. Liu, Y. Tang, C.F. Shao, P. Gong, J. Liu, S. Zhang, L. Guo, Z. Liu. *Chem. Asian J.*, 13, 1500 (2018).
[33] M.Q. Wang, L.X. Gao, Y.F. Yang, X.N. Xiong, Z.Y. Zheng, S. Li, Y. Wu, L.L. Ma. *Tetrahedron Lett.*, 57, 504 (2016).
[34] A.K. Das, H. Ihmels, S. Kölsch. *Photochem. Photobiol. Sci.*, 18, 1373 (2019).
[35] Y. Ozkay, I. Işikdağ, Z. Incesu, G. Akalin. *Eur. J. Med. Chem.*, 45, 3320 (2010).
[36] H.M. Refaat. *Eur. J. Med. Chem.*, 45, 2949 (2010).
[37] S.B. Jensen, S.J. Rodger, M.D. Spicer. *J. Organomet. Chem.*, 556, 151 (1998).
[38] R. Dheepika, R. Abhijna Krishna, P.M. Imran, S. Nagarajan. *RSC Adv.*, 10, 13043 (2020).
[39] R. Dheepika, S. Srinita, P.M. Imran, S. Nagarajan. *J. Mater. Chem. C*, 6, 6916 (2018).
[40] K. Jeyalakshmi, J. Haribabu, C. Balachandran, N.S.P. Bhuvanesh, N. Emi, R. Karvembu. *New J. Chem.*, 41, 2672 (2017).
[41] A. Wolfe, G.H. Shimer, T. Meehan. *Biochemistry*, 26, 6392 (1987).
[42] A. Reisis, M. Mureşeanu. *J. Chil. Chem. Soc.*, 57, 1409 (2012).
[43] B.C. Wang, H.R. Liao, J.C. Chang, L. Chen, J.T. Yeh. *J. Lumin.*, 124, 333 (2007).
[44] D.S. Raja, N.S.P. Bhuvanesh, K. Natarajan. *Eur. J. Med. Chem.*, 46, 4584 (2011).
[45] M. Eriksson, M. Leijon, C. Hiort, B. Nordén, A. Gräslund. *Biochemistry*, 33, 5031 (1994).
[46] V.O. Yadhukrishnan, M. Muralisankar, R. Dheepika, R. Konakanchi, N.S.P. Bhuvanesh, S. Nagarajan. *J. Coord. Chem.*, 1, 1 (2020).
[47] G.B. Jiang, W.Y. Zhang, M. He, Y.Y. Gu, L. Bai, Y.J. Wang, Q.Y. Yi, F. Du. *Spectrochim. Acta A Mol. Biomol. Spectrosc.*, 227, 117534 (2020).
[48] M. Muralisankar, R. Dheepika, J. Haribabu, C. Balachandran, S. Aoki, N.S.P. Bhuvanesh, S. Nagarajan. *ACS Omega*, 4, 11712 (2019).
[49] C. Turro, S.H. Bossmann, Y. Jenkins, J.K. Barton, N.J. Turro. *J. Am. Chem. Soc.*, 117, 9026 (1995).
[50] S. Ghosh, P. Kundu, B.K. Paul, N. Chattopadhyay. *RSC Adv.*, 4, 63549 (2014).
[51] B.J. Pages, D.L. Ang, E.P. Wright, J.R.A. Wright. *Dalton Trans.*, 44, 3505 (2015).
[52] K.K. Patel, E.A. Plummer, M. Darwish, A. Rodger, M.J. Hannon. *J. Inorg. Biochem.*, 91, 220 (2002).